BULLETIN OF THE POLISH ACADEMY OF SCIENCES
TECHNICAL SCIENCES, Vol. 70(2), 2022, Article number: e140353
DOI: 10.24425/bpasts.2022.140353

Lyapunov stability based sliding mode observer for sensorless control of permanent magnet synchronous motor

NAVANEETHAN Soundirarajan[1]*, KANTHALAKSHMI Srinivasan[2], and AANDREW BAGGIO S.[1]

[1] Department of Instrumentation and Control Systems Engineering, PSG College of Technology, Coimbatore-641004, Tamilnadu, India
[2] Department of Electrical and Electronics Engineering, PSG College of Technology, Coimbatore-641004, Tamilnadu, India

Abstract. In recent years there has been an increasing demand for electric vehicles due to their attractive features including low pollution and increase in efficiency. Electric vehicles use electric motors as primary motion elements and permanent magnet machines found a proven record of use in electric vehicles. Permanent magnet synchronous motor (PMSM) as electric propulsion in electric vehicles supersedes the performance compared to other motor types. However, in order to eliminate the cumbersome mechanical sensors used for feedback, sensorless control of motors has been proposed. This paper proposes the design of sliding mode observer (SMO) based on Lyapunov stability for sensorless control of PMSM. The designed observer is modeled with a simulated PMSM model to evaluate the tracking efficiency of the observer. Further, the SMO is coded using MATLAB/Xilinx block models to investigate the performance at real-time.

Key words: electric vehicles; permanent magnet synchronous motor; sensorless control; sliding mode observer; Lyapunov stability; tracking efficiency.

1. INTRODUCTION

With the known potential advantages including low operating cost and lesser internal components, electric vehicles (EVs) are possible alternate to traditional internal combustion (IC) engine based vehicles. Permanent magnet synchronous motor (PMSM) possesses numerous merits such as better torque to volume ratio and increased efficiency in order to find its place in EV technology. Attempts are made to design robust control using fuzzy inference system with smooth inverse based dead-zone compensation [1]. Sliding mode controllers with novel reaching laws are developed to obtain better response even in the presence of uncertainties [2]. A modified direct torque control (DTC) is proposed with stator resistance estimator to provide good dynamic performance. A robust speed controller, H∞ controller with Smith predictor is implemented to improve the speed control performance of PMSM [3]. An observer works similarly to a controller but it strives to make the error between the measured outputs and its estimated outputs zero [4]. The closed loop system relies on rotor speed feedback in order to generate control signal [5]. Usually, Hall sensors and rotary encoders are employed to measure rotor speed of PMSM. These mechanical sensors are often bulky and need excitation to perform sensing operation [6]. They also occupy more space in the rotor and need frequent maintenance. Thus observer strategies are proposed by researchers to tackle the above said issues [7]. The linear observers including extended Kalman filter derivatives are able to observe a state variable which is linear in nature and when a system is nonlinear there exists a need for a nonlinear observer [8]. An estimator using model reference adaptive system (MRAS) is implemented to observer rotor speed. MRAS uses a pre patterned frequency of signal is applied to the position and velocity estimator implemented in feedback loop of the PMSM servo system [9]. The sensorless operation of PMSM servo drive using high speed sliding mode observer (SMO) is implemented [10, 11]. A sensorless control of interior PMSM using current derivative approach with a recursive least square (RLS) estimator is used with a torque and flux observer. This composite observer brings the possibility of estimating running speed as well as speed at standstill [12]. A reduced order nonlinear observer is introduced to estimate motor speed by measuring only voltages and currents [13]. The sensorless control employing sliding mode observer has intentional saturation to limit chattering. A robust SMO using two phase currents provides good dynamic performance in mid and low range speeds [14]. An improved estimator is implemented using terminal mode SMO [15].

The remainder of this paper is organized as follows: Section 2 presents mathematical model of PMSM in d-q axis frame derived using governing equations. A design procedure of closed loop control of PMSM using exponential reaching law based on sliding mode control (SMC) is derived in Section 3. Mathematical model of sliding mode observer (SMO) and design of SMO based on Lyapunov function is given in Section 4. Simulation results are briefed in Section 5 and in Section 6 elucidate hardware implementation details are followed by the conclusion.

*e-mail: snn.ice@psgtech.ac.in

Manuscript submitted 2021-08-09, revised 2021-12-08, initially accepted for publication 2021-12-26, published in April 2022.

© 2022 The Author(s). This is an open access article under the CC BY license (http://creativecommons.org/licenses/by/4.0/)

2. MODELING OF PMSM

A good observer model indeed requires a good plant model. In order to develop PMSM model the following assumptions are made [16]

1. The induced electro motive force (EMF) is sinusoidal.
2. The rotor is non-salient.
3. Eddy currents and hysteresis losses are negligible.

The PMSM model is developed in d-q axis frame using first principle. Modelling in d-q frame has numerous advantages including simplicity in analysis, application of vector control for controlling speed as well as torque separately and also it offers provision of disturbance decoupling in systems. This is accomplished by converting actual machine parameters into two phase parameters (using Park transformation). Two state currents namely direct and quadrature axes and also the angular velocity (rotor speed) of the machine are the state variables. The voltage applied to direct and quadrature axes are the control variables. The electrical equivalent circuits are given in Fig. 1.

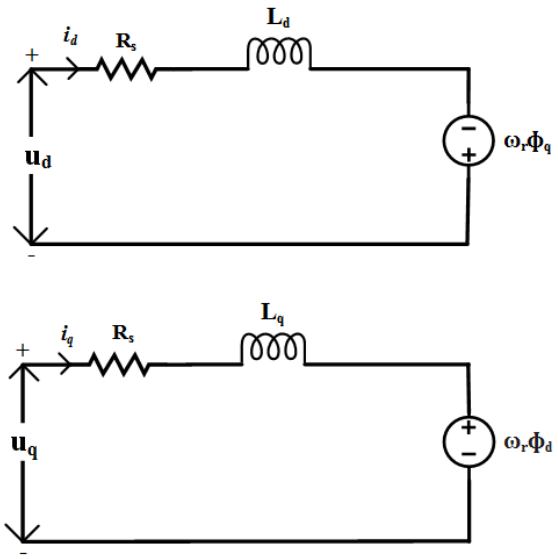

Fig. 1. Electrical equivalent circuit

The PMSM model with three state variables are obtained using first principle equations as given in (1)–(3)

$$\frac{di_d}{dt} = \frac{1}{L_d}\left[u_d - R_s i_d + n_p \omega i_q\right], \tag{1}$$

$$\frac{di_q}{dt} = \frac{1}{L_q}\left[u_q - R_s i_q - n_p \omega i_d - \frac{n_p \phi_v \omega}{L_q}\right], \tag{2}$$

$$\frac{d\omega}{dt} = \frac{1}{J}\left[K_t i_q - B\omega - T_L\right]. \tag{3}$$

The torque developed in the motor is given by

$$T_e = \frac{3}{2}\left(\frac{n_p}{2}\right)\left(\phi_d i_q - \phi_q i_d\right), \tag{4}$$

where,

i_d and i_q are d-q stator currents,
L_d and L_q are d-q axes inductances,
u_d and u_q are d-q axes input voltages,
ϕ_v is rotor flux linkage,
ω is rotor speed,
R_s is resistance of the windings,
T_e is electromagnetic torque,
T_L is load torque,
ϕ_d is direct axis flux linkage,
ϕ_q is quadrature axis flux linkage,
J is moment of inertia,
B is friction co-efficient.

3. CONTROLLER DESIGN

The cascaded closed loop PMSM control system has two loops having two inner loop current controllers and one outer loop speed controller. The inner loop current controllers use proportional integral (PI) controllers and outer loop speed controller designed using advanced controller. The simplified control scheme of PMSM is given in Fig. 2. The schematic representation keeps simple PI controllers in both currents and speed loop.

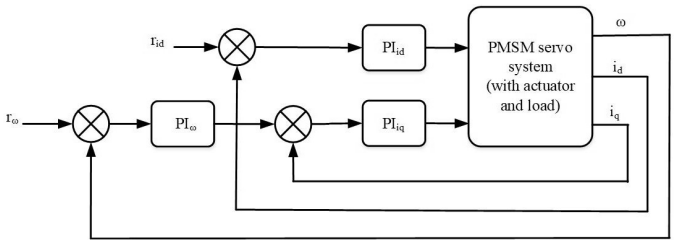

Fig. 2. Simplified control scheme

Compared with other nonlinear control methods, SMC is more insensitive to internal parameter variations and external disturbance once the system trajectory reaches and stays on the sliding surface [17]. However, the design of SMC controller with reduced chattering is crucial [18] and this motivates the researches for a new reaching law [19]. A closed loop speed controller is designed using SMC. The control objective is to track reference set in the outer loop speed controller. The design of speed controller using sliding mode involves two steps namely reaching law design and control law design, the first step is to choose the sliding-mode surface, and the next step is to design the control input such that the system trajectory is forced toward the sliding-mode surface, which ensures the system to satisfy the sliding-mode reaching condition.

Exponential reaching law based SMC is designed in speed loop [20]. The novel sliding mode reaching law is realized based on the choice of an exponential term that adapts to the variations of the sliding-mode surface and system states [21]. The exponential reaching law based SMC has been derived as follows.

A general nonlinear model representing the system is taken as

$$\begin{aligned} \dot{x_1} &= x_2\,, \\ \dot{x_2} &= f(x) + g(x) + b(x)u\,, \end{aligned} \tag{5}$$

where x is the system state vector, $g(x)$ represents the provision to add system disturbances, $b(x)$ is a non zero input matrix and u is the control input.

The typical sliding-mode surface is chosen with state variables x_1 and x_2 as follows:

$$s = cx_1 + x_2\,. \tag{6}$$

The aim of this design phase is to design a control input u in such a way that the sliding-mode reaching condition is met. The sliding surface with equal reaching law or conventional reaching law is chosen as follows:

$$\dot{s} = -k \cdot \mathrm{sgn}(s), \tag{7}$$

A modification in reaching law i.e., exponential reaching is chosen in order to make the convergence faster. The sliding surface with exponential reaching law is

$$\dot{s} = -eq(x_1, s) \cdot \mathrm{sgn}(s), \tag{8}$$

where $eq(x_1, s)$ is $\dfrac{k}{\varepsilon + (1 + \dfrac{1}{(|x_1| - \varepsilon)e^{-\delta|s|}})}$.

Here ε and δ are design parameters. The subsequent step is to design the control input such that the system trajectory is forced toward the sliding-mode surface, which ensures the system to satisfy the sliding-mode reaching condition. Speed controller is designed based on different reaching laws. Consider,

$$s = e = \omega_{\mathrm{ref}} - \omega\,. \tag{9}$$

Equation (9) is called linear sliding-mode surface. Taking the time derivative of the sliding-mode surface yields

$$\dot{s} = \dot{e} = \dot{\omega_{\mathrm{ref}}} - \dot{\omega}\,. \tag{10}$$

The dynamic equation of the motor can be expressed as follows:

$$\begin{aligned} &a_n i_q - b_n T_L - c_n \omega + \Delta a i_q - \Delta b T_L - \Delta c \omega \\ &\quad = a_n i_q - c_n \omega + r(t), \end{aligned} \tag{11}$$

where,

$$\begin{aligned} a &= a_n + \Delta a = \frac{3 n_p \phi_v}{2J}\,, \\ b &= b_n + \Delta b = \frac{n_p}{2J}\,, \\ c &= c_n + \Delta c = \frac{B}{J}\,, \\ r(t) &= \Delta a i_q - \Delta c \omega - b T_L \quad \text{and} \quad |r(t)| \le t. \end{aligned}$$

Therefore,

$$\dot{s} = \dot{\omega_{\mathrm{ref}}} + c_n \omega - r(t) - a_n i_q = -k \cdot \mathrm{sgn}(s). \tag{12}$$

The speed controller generates a reference signal (i_q^*) to inner loop current control. Thus, a speed controller employing exponential reaching law is given as

$$i_q^* = a_n^{-1} \left\{ \dot{\omega}_{\mathrm{ref}} + c_n \omega + [l + eq(x_1, s)] \,\mathrm{sgn}(s) \right\}, \tag{13}$$

where, l is upper bound of lumped disturbances, x_1 is error state variable, k is sliding mode gain and ω_{ref} is reference speed and s is sliding surface consisting of error dynamics. a_n and c_n are the new constants introduced which are equivalent to a and c respectively. The exponential reaching law promises to have faster reaching time with limited chattering.

4. SLIDING MODE OBSERVER

As the mechanical sensors used for speed measurements are often bulky and need frequent maintenance, there arises a need for sensorless control scheme. In this regard, the speed observer based closed loop PMSM system serves the need. As the system state equations (1) and (2) involves nonlinear terms, a nonlinear observer i.e., sliding mode observer (SMO) is implemented to obtain sensorless control scheme.

A SMO uses nonlinear signals to drive its estimated states nearer to the measured states [22, 23]. The SMO is derived by Lyapunov stability concept for systems. The SMO is able to capture the system dynamics and smoothened by the measured states [24]. The closed loop vector control of PMSM with SMO is shown in Fig. 3. Since the speed of the rotor is strongly influenced by the quadrature axis current, its estimation error is used to control the estimation of the speed. Though various researchers attempt to implement SMO and improvement in SMO which are based on creating new sliding surface, this algorithm uses the existing mathematical model of plant and switching terms for estimation. The stability of switching is further ensured by Lyapunov stabilty.

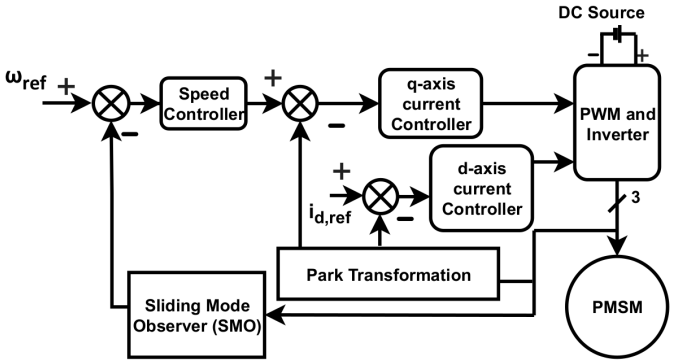

Fig. 3. Vector control of PMSM with Sliding Mode Observer

4.1. Model of PMSM with SMO

The SMO model resembles the PMSM model except for the additional switching terms which ensure that the estimation errors remain bounded. The estimated state variables i.e., direct axis current, quadrature axis current and angular velocity are obtained with actual state and estimation error ($\hat{i_d} = i_d - \bar{i_d}$, $\hat{i_q} = i_q - \bar{i_q}$, $\hat{\omega} = \omega - \bar{\omega}$). The actual state model available in equations (1)–(3) is subtracted from estimation error of respective state quantities to obtain the speed estimation using SMO

as follows:

$$\dot{\hat{\omega}} = \frac{1}{J}\left[K_t(i_q - \bar{i_q}) - B(\omega - \bar{\omega}) - T_L\right] + K_1 \text{sign}(\bar{\omega}) \tag{14}$$

rewriting (14) as

$$\dot{\hat{\omega}} = a_1 \hat{i_q} - a_2 \hat{\omega} - \frac{T_L}{J} + K_1 \text{sign}(\bar{\omega}). \tag{15}$$

Similarly the direct and qudarature axis current estimations are given in (16) and (17)

$$\dot{\hat{i_d}} = -a_3 \hat{i_d} + n_p \hat{\omega} \hat{i_q} + \frac{V_d}{L_d} + K_2 \text{sign}(\bar{i_d}), \tag{16}$$

$$\dot{\hat{i_q}} = -a_4 \hat{i_q} - n_p \hat{\omega} \hat{i_d} - a_5 \hat{\omega} + \frac{V_q}{L_q} + K_3 \text{sign}(\bar{i_q}) \tag{17}$$

where,

$$a_1 = \frac{K_t}{J}; \quad a_2 = \frac{B}{J}; \quad a_3 = \frac{R_s}{L_d}; \quad a_4 = \frac{R_s}{L_q}; \quad a_5 = \frac{n_p \phi_v}{L_q};$$

$$\bar{i_d} = i_d - \hat{i_d}; \quad \bar{i_q} = i_q - \hat{i_q}; \quad \bar{\omega} = \omega - \hat{\omega}.$$

4.2. SMO error model

The error model equations are obtained by subtracting the SMO model equations from the PMSM model

$$\dot{\bar{\omega}} = a_1 \dot{\bar{i_q}} - a_2 \bar{\omega} - \frac{T_L}{J} - K_1 \text{sign}(\bar{\omega}), \tag{18}$$

$$\dot{\bar{i_d}} = -a_3 \bar{i_d} + n_p \left(\omega i_q - \hat{\omega} \hat{i_q}\right) - K_2 \text{sign}(\bar{i_d}), \tag{19}$$

$$\dot{\bar{i_q}} = -a_4 \bar{i_q} - n_p \left(\omega i_d - \hat{\omega} \hat{i_d}\right) - a_5 \hat{\omega} - K_3 \text{sign}(\bar{i_q}). \tag{20}$$

The switching coefficients are derived using Lyapunov stability concept. The closed loop sensorless control of PMSM with SMO is given in Fig. 3.

4.3. Design of SMO based on Lyapunov function

The Lyapunov function candidate for the error model considered as:

$$V = \frac{1}{2}\left(\bar{i_d}^2 + \bar{i_q}^2 + \omega^2\right). \tag{21}$$

It can be seen that $V(0) = 0$, $V > 0$ (positive definite) when $i_d \neq 0$, $i_q \neq 0$ and $\omega \neq 0$ and $V \to \infty$ as $(i_d, i_q, \omega) \to \infty$ (radially unbounded) and hence V can be considered as a Lyapunov function of the error model. A system′s Lyapunov function acts as an indicator of the stability of a particular state of the system [25–27]. If V is negative definite, the corresponding state is said to be asymptotically stable. Hence, to check the stability of the system's origin (where the state errors are zero) and to find out the conditions (region of attraction) under which the trajectories will asymptotically converge to the origin, V is computed as

$$\begin{aligned}\dot{V} = &\left(-a_3 \bar{i_d} + n_p \left(\omega i_q - \hat{\omega} \hat{i_q}\right) - K_2 \text{sign}(\bar{i_d})\right) * \bar{i_d} \\ &\left(-a_4 \bar{i_q} + n_p \left(\omega i_d - \hat{\omega} \hat{i_d}\right) - a_5 \bar{\omega} - K_3 \text{sign}(\bar{i_q})\right) * \bar{i_q} \\ &\left(a_1 \bar{i_q} - a_2 \bar{\omega} - \frac{T_L}{J} - K_1 \text{sign}(\bar{i_q})\right) * \bar{\omega}.\end{aligned} \tag{22}$$

Rearranging (22) gives

$$\begin{aligned}\dot{V} = &-a_3 \bar{i_d}^2 - a_4 \bar{i_q}^2 - a_2 \bar{\omega}^2 + \left(n_p \left(\omega i_q - \hat{\omega} \hat{i_q}\right) \bar{i_d}\right. \\ &- \left(n_p (\omega i_d - \hat{\omega} \hat{i_d}) \bar{i_q}\right) - (a_1 - a_5) \bar{\omega} \bar{i_q} + (-K_1 \text{sign}(\bar{i_q}) * \bar{\omega} \\ &- K_2 \text{sign}(\bar{i_d}) * \bar{i_d} - K_3 \text{sign}(\bar{i_q})) * \bar{i_q}) - \frac{T_L}{J} * \bar{\omega}.\end{aligned} \tag{23}$$

Introducing a new constant $a_1 - a_5 = a_6$ in (23) and considering no load condition ($T_L = 0$) gives

$$\begin{aligned}\dot{V} = &(-a_3 \bar{i_d}^2 - a_4 \bar{i_q}^2 - a_2 \bar{\omega}^2 + \left(n_p (\omega i_q - \hat{\omega} \hat{i_q}) \bar{i_d}\right. \\ &- \left(n_p \left(\omega i_d - \hat{\omega} \hat{i_d}\right) \bar{i_q}\right) - (a_6) \bar{\omega} \bar{i_q} + (-K_1 \text{sign}(\bar{i_q}) * \bar{\omega} \\ &- K_2 \text{sign}(\bar{i_d}) * \bar{i_d} - K_3 \text{sign}(\bar{i_q})) * \bar{i_q}).\end{aligned} \tag{24}$$

Simplification of the terms in the second bracket in (24) gives

$$\begin{aligned}&n_p \left(\omega i_q - \hat{\omega} \hat{i_q}\right) \bar{i_d} - \left(n_p \left(\omega i_d - \hat{\omega} \hat{i_d}\right) \bar{i_q}\right) \\ &= n_p \left(\omega i_q - \hat{\omega} \hat{i_q} + \omega \hat{i_q} - \omega \hat{i_q}\right) - \hat{\omega} \hat{i_q} \bar{i_d} \\ &n_p \left(\omega i_d - \hat{\omega} \hat{i_d} + \omega \hat{i_d} - \omega \hat{i_d}\right) - \hat{\omega} \hat{i_d} \bar{i_q}.\end{aligned} \tag{25}$$

Doing algebraic manipulation provides

$$\begin{aligned}&n_p \left(\omega i_q - \hat{\omega} \hat{i_q}\right) \bar{i_d} - \left(n_p \left(\omega i_d - \hat{\omega} \hat{i_d}\right) \bar{i_q}\right. \\ &= n_p \bar{\omega} \hat{i_q} \bar{i_d} - n_p \bar{\omega} \hat{i_d} \hat{i_q}.\end{aligned} \tag{26}$$

Substituting (26) into (25) gives,

$$\begin{aligned}\dot{V} = &\left(-a_3 \bar{i_d}^2 - a_4 \bar{i_q}^2 - a_2 \bar{\omega}^2\right) + \left(n_p \bar{\omega} \hat{i_q} \bar{i_d} - n_p \bar{\omega} \hat{i_d} \bar{i_q}\right) \\ &+ (a_6) \bar{\omega} \bar{i_q} - K_1 \text{sign}(\bar{i_q}) * \bar{\omega} - K_2 \text{sign}(\bar{i_d}) * \bar{i_d} \\ &- K_3 \text{sign}(\bar{i_q}) * \bar{i_q}\end{aligned} \tag{27}$$

Rearranging (27) gives,

$$\begin{aligned}\dot{V} = &\left(-a_3 \bar{i_d}^2 - a_4 \bar{i_q}^2 - a_2 \bar{\omega}^2\right) + \left(n_p \bar{\omega} \hat{i_q} \bar{i_d} - K_2 \text{sign}(\bar{i_d}) * \bar{i_d}\right) \\ &+ (a_6 \bar{\omega} \bar{i_q} - K_1 \text{sign}(\bar{i_q}) * \bar{\omega}) \\ &+ \left(-n_p \bar{\omega} \hat{i_d} \bar{i_q} - K_3 \text{sign}(\bar{i_q}) * \bar{i_q}\right).\end{aligned} \tag{28}$$

For the error dynamics to reach the origin, it should be negative definite. This implies that the right hand side of (24) should always be less than zero. The first three terms are always negative as they are quadratic terms and have a negative sign and hence they need not be bothered with. The other terms are paired up with suitable switching terms which are chosen in such a way that the equation remains negative definite. The pairings are given as follows

$$\begin{aligned}a_6 \bar{\omega} \bar{i_q} - K_1 \text{sign}(\bar{i_q}) * \bar{\omega} < 0, \\ n_p \bar{\omega} \hat{i_q} \bar{i_d} - K_2 \text{sign}(\bar{i_d}) * \bar{i_d} < 0, \\ -n_p \bar{\omega} \hat{i_d} \bar{i_q} - K_3 \text{sign}(\bar{i_q}) * \bar{i_q} < 0.\end{aligned}$$

Solving to obtain switching constants as follows

$$K_1 > a_6 |\bar{i_q}|; \quad K_2 > \frac{n_p \bar{\omega} \hat{i_q}}{\text{sign}(\bar{i_d})}; \quad K_3 > \frac{-n_p \bar{\omega} \hat{i_d}}{\text{sign}(\bar{i_q})}.$$

Assuming that the observer's estimated values will not exceed the physical bounds of the machine, it can be stated that the maximum error will be within the bounds.

$$|\bar{\omega}| \leq |\omega_{\max}|.$$

Since $i_s = \sqrt{i_d^2 + i_q^2}$ the errors $\bar{i_d}$ and $\bar{i_q}$ are assumed to have an upper bound of $i_{s,\max}$ and a lower bound of $-i_{s,\max}$

$$|\bar{i_d}| \leq |i_{s,\max}|,$$

$$|\bar{i_q}| \leq |i_{s,\max}|.$$

Thus the values of K_1, K_2 and K_3 are obtained as

$$K_1 > a_6|i_{s,\max}|; \quad K_2 > n_p\omega_{\max}i_{s,\max}; \quad K_3 > n_p\omega_{\max}i_{s,\max}.$$

Since the signs of the errors can change, the absolute value of the terms is considered so that the selected switching constants always satisfy the constraints.

5. SIMULATION RESULTS

The closed loop system with SMO is simulated using MATLAB/Simulink. The parameters used in mathematical model of PMSM, controller design and observer design are given in Table 1.

Table 1
Simulation parameters

Parameters	Values
Stator resistance R_s	1.74 Ω
Inductance L_d	0.0066 H
Inductance L_q	0.0058 H
Rotor flux ϕ_v	0.1546 V/rad/s
Moment of inertia J	0.00176 kgm^2
Friction visicious gain B	0.00038818 Nm/rad/s
Number of pole pairs n_p	3
Rated speed	4000 rpm
Sliding mode gain of controller k	22
Exponential reaching law design parameters ε and δ	0.2 and 10
Switching constant K_1 (101% of bound)	95.71
Switching constant K_2 (101% of bound)	202
Switching constant K_3 (101% of bound)	202

5.1. Estimation of rotor angular velocity

The estimation of state variables in SMO needs measured current signals (direct axis current and quadrature axis current). The SMO estimates the rotor speed using the current signals. The closed loop PMSM uses the estimated rotor speed in the speed loop as if it is the actual rotor speed. The controller based on sliding mode using exponential reaching law has been used for speed control and inner loop current loops use the PI controllers. Figure 4 shows the estimated and actual rotor speed.

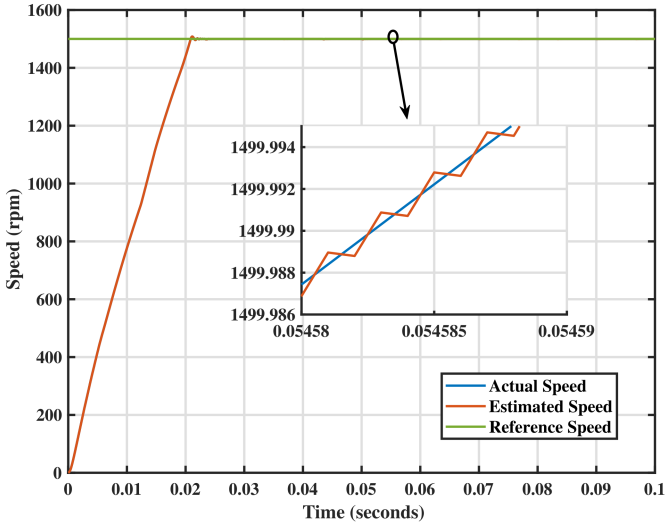

Fig. 4. Estimated and actual rotor speed

It is seen that both estimated and actual speed tracks the reference speed. The very low difference between the estimated and actual rotor speed implies that the SMO observes the dynamics better and the unmeasured state can be observed with the available measurements. Though the estimation technique does not use the actual rotor speed information to process the observer, the actual rotor speed which is available from closed loop PMSM servo system is being used to compare with the estimated values. The overall system takes around 0.02s to reach the steady state and no significant overshoot is seen in Fig. 4 The difference between actual and estimated rotor speed is calculated and plotted Fig. 5 shows the estimation error of SMO.

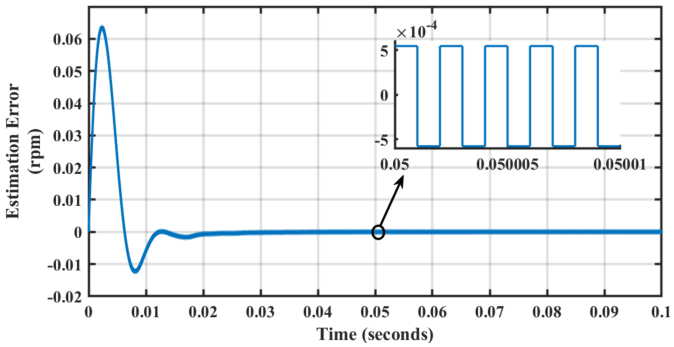

Fig. 5. Estimation error of SMO

An initial overshoot of 0.712 rpm is observed with the error chattering between $-3.15 \cdot 10^{-3}$ and $+3.15 \cdot 10^{-3}$ rpm at steady state which has been obtained at 49 ms. It is seen that the estimation error increases initially till the error reaches the sliding manifold of the observer plane. As the time progresses the estimator is able to capture the dynamics and goes along with the actual speed. Thus the estimation error reaches almost

zero. Right from the time instant 0.015 s there exists a very negligible constant estimation error which ranges from $-5 \cdot 10^{-4}$ to $+5 \cdot 10^{-4}$ which can′t be quenched as the property of a sliding nature of the observer.

5.2. Estimation of d and q axis currents

Further, the performance of SMO is evaluated for smoothing the outputs of direct and quadrature axis currents i.e., the estimated values of currents are compared with the actual currents. From Fig. 6, it is seen that the estimated values of direct and quadrature axis currents track the actual currents. Though the currents are measurable it is possible to estimate the measured states and then be compared with actual currents. The SMO tries to bring this estimation error to near zero in order to ensure better observing capability. In addition to this, a fast varying noise is deliberately added to measured currents to evaluate the performance of this observer. The tracking performance of SMO is further analyzed with load changes. The load torque is intentionally added into the PMSM closed loop system during a specific time period and thus the performance is analysed and given in Fig. 6.

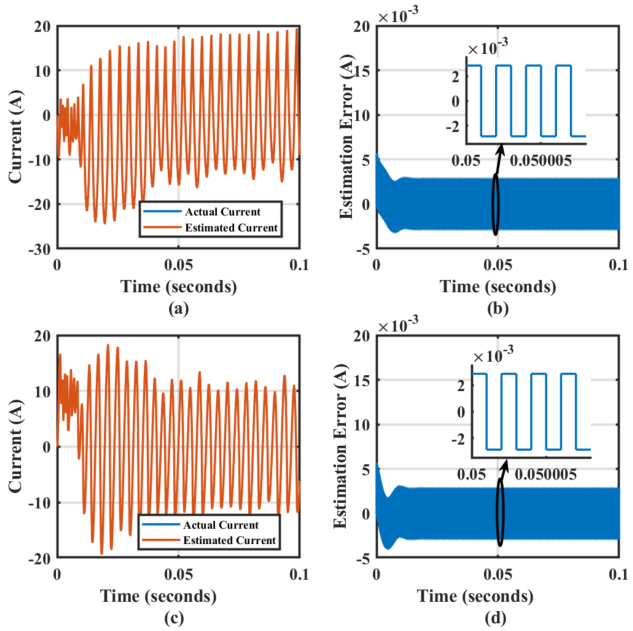

Fig. 6. Estimation of currents: (a) direct axis current, (b) estimation error of direct axis current, (c) quadrature axis current, (d) estimation error of quadrature axis current

6. HARDWARE IMPLEMENTATION

The controller and observer algorithms are coded in Matlab/Simulink-Xilinx loaded personal computer (PC). The program is then converted to a .bin file which is loaded to FPGA controller. The controller takes information of rotary encoder as well as voltage and currents of the supply to the machine. The motor is attached with a mechanical loading arrangement. The controller also communicates the status information to the PC. The PC is also loaded with a front end online monitoring system called WAVECT. The necessary inputs including controller gains, direction of rotation, reference inputs are provided in the front panel. The output in numerical as well as graphical information by means of plot is available at the front end of the software. Figure 7 shows the PMSM test bed. Programming in Matlab-Simulink Xilinx includes application-specific blocks for writing the commutation logic for inverter setup. The program uses block sets available in Matlab/Simulink-Xilinx. The sliding mode control with exponential reaching law in closed loop controller is implemented. In order to implement sensorless control scheme of PMSM in hardware test bed, the sliding mode observer (SMO) is coded in Matlab/Simulink-Xilinx Platform. The real time data is loaded to the SMO algorithm. The estimation response is obtained from SMO in offline.

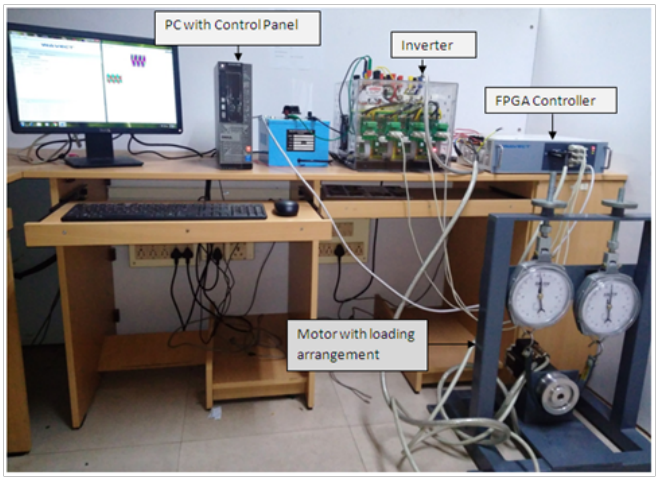

Fig. 7. Experimental setup of PMSM drive

6.1. Estimation of speed

The SMO algorithm is coded in *d*-*q* axis frame. The measured three phase currents i.e., Ia, Ib and Ic are converted to *d*-*q* axis currents using Park transformation. The measured angular velocity using encoder is then used to compare the performance of SMO. The estimated and actual speed plots of PMSM are shown in Fig. 8. It is seen from Fig. 8 that the real time SMO algorithm is able to estimate the speed of PMSM as the estimation error is negligible. Thus the SMO is able to capture the original

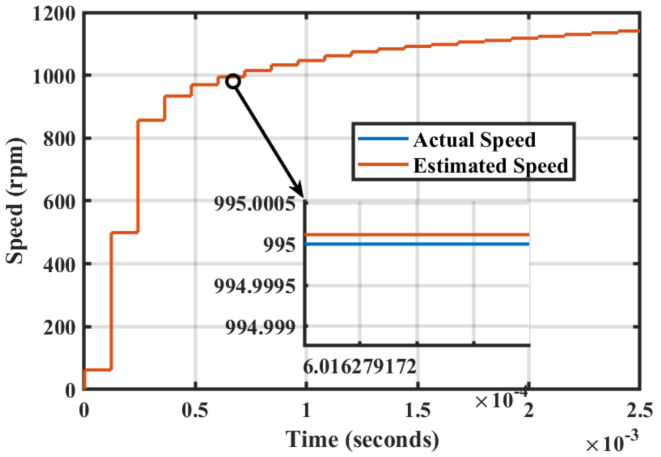

Fig. 8. Estimation of speed using SMO

system dynamics and mimic the performance of PMSM servo system. The estimation is done offline with signal data obtained from hardware setup. The data are fed to Xilinx platform to account the delay time encountered in real-time.

6.2. Estimation of currents

Similarly the direct and quadrature currents are estimated using real time coded SMO in Matlab/Xilinx. As the SMO incorporates all the state varibales it is possible to estimate the original measured variable and smooth the output from the current sensors. The estimated direct and quadrature axis currents are shown in Fig. 9.

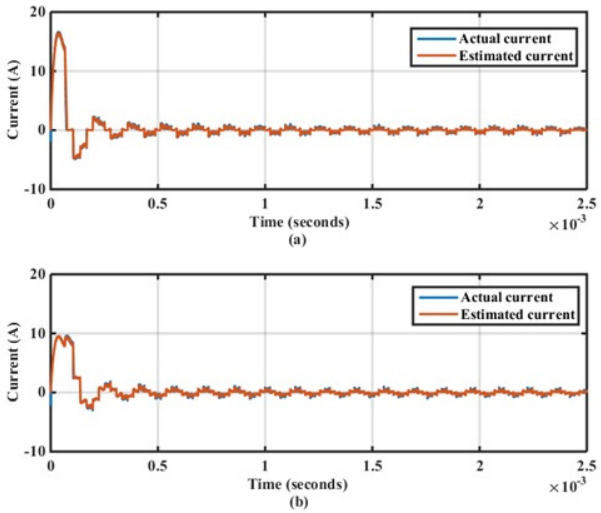

Fig. 9. Estimation of currents using SMO: (a) direct current, (b) quadrature current

As observed through Fig. 9, the estimated direct and quadrature currents follow the measured currents. The estimated currents are able to mimic the dynamics of the actual currents with negligible error.

7. CONCLUSION

A robust nonlinear control algorithm i.e., SMC is designed to deliver robust performance in PMSM servo systems under uncertain disturbances and parameter variations. The design of SMC involves two steps namely reaching phase and controller design. The design of SMC is improved in its reaching phase i.e exponential reaching law. This reaching law gives a good reaching time along with very less chattering. Motion control systems use speed feedback information in order to generate control signal. The need for sensorless control arises when there is a difficulty to accommodate the bulky mechanical sensors in the closed loop system. Soft sensing, in other words, the sensorless control, makes the system to use less reliable sensors thus eliminates the unreliable measurements. The developed SMO uses existing plant model and Lyapunov stability concept for estimation of state variables. In speed estimation, the measured direct and quadrature axis currents are fed as input to the SMO and the rotor speed is the targeted output of the estimator. The simulation results prove the good estimation accuracy of SMO. The algorithm is further coded in hardware platform and real-time data are provided to evaluate the performance.

REFERENCES

[1] X. Wang and S. Wang, "Adaptive fuzzy robust control of PMSM with smooth inverse based dead-zone compensation," *Int. J. Control. Autom. Syst.*, vol. 14, no. 2, pp. 378–388, 2016, doi: 10.1007/s12555-015-0010-6.

[2] A.K. Junejo, W. Xu, C. Mu, M.M. Ismail, and Y. Liu, "Adaptive Speed Control of PMSM Drive System Based a New Sliding-Mode Reaching Law," *IEEE Trans. Power Electron.*, vol. 35, no. 11, pp. 12110–12121, 2020, doi: 10.1109/TPEL.2020.298689.

[3] A.M.O Anwer, F.A. Omar, and A.A. Kulaksiz, "Design of a Fuzzy Logic-based MPPT Controller for a PV System Employing Sensorless Control of MRAS-based PMSM," *Int. J. Control. Autom. Syst.*, vol. 18, no. 11, pp. 2788–2797, 2020, doi: 10.1007/s12555-019-0512-8.

[4] W.H. Chen, "Disturbance observer based control for nonlinear systems," *IEEE/ASME Trans. Mechatron.*, vol. 9, no. 4, pp. 706–710, 2004, doi: 10.1109/TMECH.2004.839034.

[5] P. Naghshtabrizi and J.P. Hespanha, "Designing an observer-based controller for a network control system," in *Proceedings of the 44th IEEE Conference on Decision and Control and the European Control Conference CDC-ECC'05*, 2005, pp. 848–853, doi: 10.1109/CDC.2005.1582263.

[6] T.D. Batzel and K.Y. Lee, "Commutation torque ripple minimization for permanent magnet synchronous machines with Hall effect position feedback," *IEEE Trans. Energy Convers.*, vol. 13, no. 3, pp. 257–262, 1998, doi: 10.1109/60.707605.

[7] J. Hu, J. Zou, F. Xu, Y. Li, and Y. Fu, "An improved PMSM rotor position sensor based on linear Hall sensors," *IEEE Trans. Magn.* vol. 48, no. 11, pp. 3591–3594, 2012, doi: 10.1109/TMAG.2012.2202279.

[8] J. Niewiara, T. Tarczewski, and L.M. Grzesiak, "Application of extended Kalman filter for estimation of periodic disturbance and velocity ripple reduction in PMSM drive," *Bull. Pol. Acad. Sci. Tech. Sci.*, vol. 68, no. 4, pp. 983–995, 2020, doi: 10.24425/bpasts.2020.134649.

[9] L.A. Jones and J.H Lang, "A State Observer for the Permanent-Magnet Synchronous Motor," *IEEE Trans. Ind. Electron.* vol. 36, no. 3, pp. 374–382, 1989, doi: 10.1109/41.31500.

[10] H. Rasmuseen, "Sensorless speed control including zero speed of non salient PM synchronous drives," *Bull. Polish Acad. Sci. Tech. Sci.*, vol. 54, no. 3, pp. 293–298, 2006.

[11] J. Yang, M. Dou, and D. Zhao, "Iterative sliding mode observer for sensorless control of five-phase permanent magnet synchronous motor," *Bull. Pol. Acad. Sci. Tech. Sci.*, vol. 65, no. 6, pp. 845–857, 2017, doi: 10.1515/bpasts-2017-0092.

[12] Y. Zhao and X. Liu, "Speed Control for PMSM Based on Sliding Mode Control With a Nonlinear Disturbance Observer," in *Proceedings – 2019 Chinese Automation Congress, CAC 2019*, 2019, pp. 634–639, doi: 10.1109/CAC48633.2019.8996376.

[13] Z.Y Zhang, L. Bao Zhang, and H. Wang, "Research on PMSM Position Sensorless Control Based on Improved Sliding Mode Observer," in *2019 22nd International Conference on Electrical Machines and Systems, ICEMS 2019*, 2019, doi: 10.1109/ICEMS.2019.8921816.

[14] A.G. Daniel, "Sliding-Mode Observer For Sensorless Control Of Permanent Magnet Synchronous Motor Drives," *J. Cont. Eng. App. Inf.*, vol. 5, no. 1, pp.27–34, 2003.

[15] S. Wu and J. Zhang, "A Terminal Sliding Mode Observer Based Robust Backstepping Sensorless Speed Control for Interior Permanent Magnet Synchronous Motor," *Int. J. Control. Autom. Syst.*, vol. 16, no. 6, pp. 2743–2753, 2018, doi: 10.1007/s12555-017-0806-7.

[16] R. Krishnan, *Electric Motor Drives: Modeling, Analysis*, Prentice-Hall, New Jersy, 2011.

[17] L. Sun, X. Zhang, L. Sun, and K. Zhao, "Nonlinear speed control for PMSM system using sliding-mode control and disturbance compensation techniques," *IEEE Trans.Power Electron.*, vol. 28, no. 3, pp. 1358-1365, 2013, doi: 10.1109/TPEL.2012.2206610.

[18] B.T. Zhang, Y.G. Pi, and Y. Luo, "Fractional order sliding-mode control based on parameters auto-tuning for velocity control of permanent magnet synchronous motor," *ISA Trans.*, vol. 51, no. 5, pp. 649–656, 2012, doi: 10.1016/j.isatra.2012.04.006.

[19] S.Z. Zhang X.L. Ma, "A PMSM sliding-mode control system based-on exponential reaching law," in Proc. *International Conference on Computational Aspects of Social Networks, CASoN'10*, 2010, pp.412–414, doi: 10.1109/CASoN.2010.100.

[20] S. Navaneethan and J. Jerome, "Speed control of Permanent Magnet Synchronous Motor using Power Reaching Law based Sliding Mode Controller," *WSEAS Trans. Syst. Control*, vol. 10 pp. 270–277, 2015.

[21] H.Wang, B. Zhou, and S. Fang, "A PMSM sliding mode control system based on exponential reaching law," *Trans. China Electr. Tech. Soc.*, vol. 24, pp. 71–77, 2009.

[22] Z. Qiao, T. Shi, Y. Wang, Y. Yan, C. Xia, and X. He, "New sliding-mode observer for position sensorless control of permanent-magnet synchronous motor," *IEEE Trans. Ind. Electron.*, vol. 60, no. 2, pp. 710–719, 2013, doi: 10.1109/TIE.2012.2206359.

[23] Y. Feng, J. Zheng, X. Yu, and N.V. Truong, "Hybrid terminal sliding-mode observer design method for a permanent-magnet synchronous motor control system," *IEEE Trans. Ind. Electron.*, vol. 56, no. 9, pp. 3424–3431, 2009, doi: 10.1109/TIE.2009.2025290.

[24] Y.S. Jung and M.G. Kim, "Sliding mode observer for sensorless control of IPMSM drives," *J. Power Electron.*, vol. 9, no. 1, pp. 117–123, 2009.

[25] A. Polyakov and L. Fridman, "Stability notions and Lyapunov functions for sliding mode control systems," *J. Franklin Inst.*, vol. 351, no. 4, pp. 1831–1865, 2014, doi: 10.1016/j.jfranklin.2014.01.002.

[26] M. Rezkallah, S.K. Sharma, A. Chandra, B. Singh, and D.R. Rousse, "Lyapunov Function and Sliding Mode Control Approach for the Solar-PV Grid Interface System," *IEEE Trans. Ind. Electron.*, vol. 64, no. 1, pp. 785–795, 2017, doi: 10.1109/TIE.2016.2607162.

[27] J. Kabzinski and P. Mosiolek, "Adaptive, nonlinear state transformation-based control of motion in presence of hard constraints," *Bull. Pol. Acad. Sci. Tech. Sci.* vol. 68, no. 5, pp. 963–971, 2020, doi: 10.24425/bpasts.2020.134653.